Article

Synchrotron X-ray Powder Diffraction and Computational Investigation of Purely Siliceous Zeolite Y under Pressure

Marek Colligan, Paul M. Forster, Anthony K. Cheetham, Yongjae Lee, Thomas Vogt, and Joseph A. Hriljac

J. Am. Chem. Soc., **2004**, 126 (38), 12015-12022• DOI: 10.1021/ja048685g • Publication Date (Web): 04 September 2004

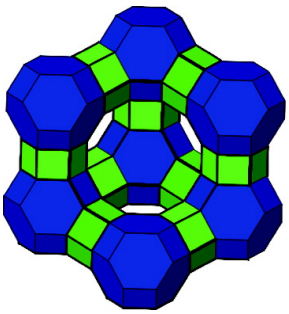

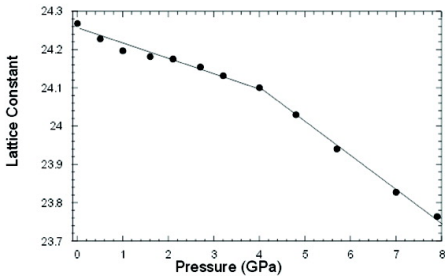

More About This Article

Additional resources and features associated with this article are available within the HTML version:

- Supporting Information
- Links to the 5 articles that cite this article, as of the time of this article download
- Access to high resolution figures
- Links to articles and content related to this article
- Copyright permission to reproduce figures and/or text from this article

View the Full Text HTML

J|A|C|S
ARTICLES
Published on Web 09/04/2004

Synchrotron X-ray Powder Diffraction and Computational Investigation of Purely Siliceous Zeolite Y under Pressure

Marek Colligan,[†] Paul M. Forster,[‡] Anthony K. Cheetham,[‡] Yongjae Lee,[§] Thomas Vogt,[§] and Joseph A. Hriljac*,[†]

Contribution from the School of Chemistry, The University of Birmingham, Birmingham, B15 2TT, United Kingdom, Materials Research Laboratory, University of California, Santa Barbara, California, and Physics Department, Brookhaven National Laboratory, Upton, New York 11973-5000

Received March 8, 2004; E-mail: j.a.hriljac@bham.ac.uk

Abstract: High-pressure synchrotron X-ray powder diffraction measurements of a sample of purely siliceous zeolite Y (faujasite) were carried out up to 8.0 GPa at room temperature using a diamond anvil cell. Measurements using silicone oil as the pressure-transmitting medium show compression of the zeolite followed by a loss of long-range ordering at 2.2 GPa. The experimentally determined bulk modulus, 38(2) GPa, is, within experimental error, identical to that of quartz. When using a methanol:ethanol:water mixture (16:3:1) as the pressure-transmitting medium, two distinct compressibility regions are observed with a dramatic change in the compression mechanism at 4 GPa. Rietveld refinement analysis of the powder patterns provides a detailed description of the underlying chemistry, with sequential pore filling the main response up to 4 GPa and framework distortions at higher pressures.

Introduction

Zeolites are nanoporous aluminosilicate materials crystallizing in a variety of low-density framework structures constructed from fully corner-connected $(Al,Si)O_4$ tetrahedra. Although the framework topology of any zeolite is determined by the particular linking arrangement of the primary tetrahedra, it is also possible to consider the structures as being composed of slightly larger assemblages, secondary building units (SBUs), such as rings or cages.[1] The $(Al,Si)O_4$ tetrahedra are rather rigid units, and it is well-known that it is the built-in flexibility of the (Al,Si)−O−(Al,Si) angle connector between these that allows zeolite structures to contract and expand in response to temperature.[2,3] These correlated changes in angles, dictated by the symmetry of the space group, correspond to distortions of the SBUs or the links between them.

Much less is know about the structural behavior of zeolites, especially that of the synthetic forms, under external pressure. However, recent studies of the natrolite,[4−7] heulendite,[8] scolecite,[9,10] bikitaite,[11] yugawaralite,[12] LTA,[13−19] FAU,[15,20,21] and RHO[22,23] systems indicate the rich possibilities for unusual pressure behavior. An excellent example is the early pioneering work by Hazen and Finger on zeolite Na−A (LTA),[13,14] a material with a void volume of nearly 50% and access to the interior controlled by 8-ring pores of ca. 4.2 Å diameter. For Na−A, it was shown that the experimentally determined volume compressibility was influenced by the nanoporosity, if the molecules of the pressure-transmitting medium that surrounded the particles were small enough to enter the pores the volume compressibility became lower than that measured with nonpenetrating fluids. The effect is substantial, the measured compressibility was nearly seven times smaller when using water instead

[†] The University of Birmingham.
[‡] University of California, Santa Barbara.
[§] Brookhaven National Laboratory.

(1) Breck, D. W. *Zeolite Molecular Sieves*; Krieger: Malabar, FL, 1984.
(2) Barrer, R. M. *Hydrothermal Chemistry of Zeolites*; Academic Press: London, 1982.
(3) Lee, Y.; Reisner, B. A.; Hanson, J. C.; Jones, G. A.; Parise, J. B.; Corbin, D. R.; Toby, B. H.; Freitag, A.; Larese, J. Z.; Kahhlenberg, V. *J. Phys. Chem.* **2001**, *B105*, 7188−7199.
(4) Belitsky, I. A.; Fursenko, B. A.; Gabuda, S. P.; Kholdeev, O. V.; Seryotkin, Yu. V. *Phys. Chem. Minerals* **1992**, *18*, 497−505.
(5) Lee, Y.; Hriljac, J. A.; Vogt, T.; Parise, J. B.; Artioli, G. *J. Am. Chem. Soc.* **2001**, *123*, 12 732−12 733.
(6) Lee, Y.; Hriljac, J. A.; Vogt, T.; Parise, J. B.; Artioli, G. *J. Am. Chem. Soc.* **2002**, *124*, 5466−5475.
(7) Lee, Y.; Hriljac, J. A.; Vogt, T.; Parise, J. B.; Hanson, J. C.; Kim, S. J. *Nature* **2002**, *420*, 485−489.
(8) Comodi, P.; Gatta, G. D.; Zanazzi, P. F. *Eur. J. Mineral.* **2001**, *13*, 497−505.
(9) Ballone, P.; Quartieri, S.; Sani, A.; Vezzalini, G. *Am. Mineral.* **2002**, *87*, 1194−1206.
(10) Comodi, P.; Gatta, G. D.; Zanazzi, P. F. *Eur. J. Mineral.* **2002**, *14*, 567−574.
(11) Ferro, O.; Quartieri, S.; Vezzalini, G.; Fois, E.; Gamba, A.; Tabacchi, G. *Am. Mineral.* **2002**, *87*, 1415−1425.
(12) Arletti, R.; Ferro, O.; Quartieri, S.; Sani, A.; Tabacchi, G.; Vezzalini, G. *Am. Mineral.* **2003**, *88*, 1416−1422.
(13) Hazen, R. M. *Science* **1983**, *219*, 1065−1067.
(14) Hazen, R. M.; Finger, L. W. *J. Appl. Phys.* **1984**, *56*, 1838−1840.
(15) Huang, Y. *J. Mater. Chem.* **1998**, *8*, 1067−1071.
(16) Secco, R. A.; Huang, Y. *J. Phys. Chem. Solids* **1999**, *60*, 999−1002.
(17) Rutter, M. D.; Takeyuki, U.; Secco, R. A.; Huang, Y.; Wang, J. *J. Phys. Chem. Solids.* **2001**, *62*, 599−605.
(18) Rutter, M. D.; Secco, R. A.; Huang, Y. *Chem. Phys. Lett.* **2000**, *331*, 189−195.
(19) Huang, Y.; Havenga, E. A. *Chem. Phys. Lett.* **2001**, *345*, 65−71.
(20) Lui, H.; Secco, R. A.; Huang, Y. *PhysChemComm.* **2001**, *8*, 1−3.
(21) Havenga, E. A.; Huang, Y.; Secco, R. A. *Mater. Res. Bull.* **2003**, *38*, 381−387.
(22) Lee, Y.; Hriljac, J. A.; Vogt, T.; Parise, J. B.; Edmundson, M. J.; Anderson, P. A.; Corbin, D. R.; Nagai, T. *J. Am. Chem. Soc.* **2001**, *123*, 8418−8419.
(23) Lee, Y.; Vogt, T.; Hriljac, J. A.; Parise, J. B. *Chem. Mater.* **2002**, *14*, 3501−3508.

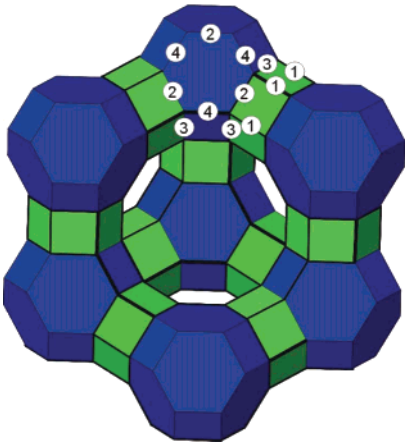

Figure 1. Faujasite (FAU) framework. The Si/Al atoms sit at the vertexes of the colored polyhedra, representative positions of oxygen atoms 1−4 are noted.

of glycerol. A second example of the affect of nanoporosity occurs in the small pore natrolite system, where reversible pressure-induced hydration occurs at around 1.5 GPa to produce a new superhydrated zeolite with a doubled water content.[4−6] For the closely related potassium gallosilicate natrolite, the pressure-induced hydration is *irreversible* and the superhydrated state remains after quenching.[7] To produce the required space in the pores for this extra water, the rigid chains that form the zeolite undergo a concerted rotation. A final example of unusual behavior occurs in the absence of a fluid pressure-transmitting medium, where pressure-induced amorphization has been reported for several zeolites with the LTA (Li−A, Na−A, K−A) and FAU (Na−X, Na−Y) structures based on powder X-ray diffraction and IR spectroscopy.[15−21] In some cases (Na−A and Na−Y), the amorphization is at least partially reversible, this "structural memory" effect has been attributed to the presence of "nondeformable" hydrated cations that can act to realign the secondary building units on decompression.[15,17,19,21]

One of the most common zeolite structures is that of zeolites X and Y, which crystallize in the faujasite (FAU) topology (Figure 1). The framework can be readily constructed from the linking of 6−6 SBUs, (double 6-rings) through 4-rings and 6-rings. This creates larger units, so-called sodalite or β-cages, that consist of 24 tetrahedra whose centers define a truncated octahedron. The β-cages are linked via 4 of the 8 hexagonal faces through the 6−6 SBUs. The resulting structure also contains larger voids, supercages, with diameters of ca. 13 Å. Access to the supercages is through 12-rings, limiting the maximum size of molecules that can enter the pores of a FAU topology zeolite to ca. 7.4 Å.

Purely siliceous Y (sil-FAU) is a synthetic zeolite that has been completely dealuminated to leave a framework consisting of pure SiO_4 tetrahedral units,[24] the framework is neutral and hydrophobic, and there are no cations or zeolitic water molecules present. It therefore provides an ideal opportunity to examine the effect of pressure on a nanoporous silicate without complications due to charge-balancing cations and their interactions with framework oxygen atoms, and the structural simplicity makes it ideal for both crystallographic and computational studies. In this paper, we report on such a combined experimental and theoretical investigation. Similar studies as a function of temperature have been highly successful, for the same sil-FAU material[25] and other purely siliceous zeolites.[26]

Experimental Section

The sample of sil-FAU was the same as used previously for neutron diffraction experiments[24] and the Na−X was obtained from Aldrich. Experiments were performed using a Diamond Anvil Cell (DAC) at the X7A beamline of the National Synchrotron Light Source (NSLS) at Brookhaven National Laboratory (BNL) and at the ID09 beamline of the European Synchrotron Research Facility (ESRF). At X7A, the primary white beam from the bending magnet is focused in the horizontal plane by a triangular, asymmetrically cut Si (220) monochromator bent to cylindrical curvature by applying a load to the center of the crystal tip, affording microfocused ($\sim$200 μm) monochromatic radiation.[27] The calibrated wavelength based on the diffraction pattern of CeO_2 was 0.66452 Å. A gas-proportional position-sensitive detector[28] was stepped in 0.25° intervals over the angular range 3.5−30° with a counting time of 60 s per step. The normalized diffraction patterns were produced using local software. At ID09, the white beam is focused by a tunable toroidal mirror and a microfocusing monochromator to a spot size of 35 μm. The calibrated wavelength based on the diffraction pattern of Si was 0.41786 Å. An image plate detector was used and an exposure time of 20 s, the normalized diffraction patterns were obtained by integrating over the whole plate using the program FIT2D.[29] The zeolite, sil-FAU or Na−X, was loaded into the DAC at ambient pressure and temperature along with a few small ruby chips and a pressure-transmitting fluid, either silicone diffusion pump oil or a methanol: ethanol:water (16:3:1) mixture. At both X-ray facilities the pressure at the sample was measured by the standard technique of detecting the shift in the R1 emission line of the included ruby chips[30] and the pressures are estimated to be accurate to ca. 0.1 GPa.

The X7A data were analyzed by individual peak fitting followed by least-squares refinement to determine accurate unit cell parameters as a function of pressure. The ID09 data (sil-FAU, alcohols/water) were of significantly higher signal-to-noise and *d*-spacing range, therefore suitable for more detailed crystallographic analysis. Rietveld structure refinements[31,32] were performed in space group $Fd\bar{3}m$ using the GSAS[33] suite of programs. Difference Fourier maps were used to locate the extraframework species found under pressure, these were included in the models as oxygen atoms. Isotropic temperature factors were refined for the framework atoms (Si, O), those of the extraframework species were fixed and the fractional site occupancies varied. Unit cell parameters and volumes are listed in Tables 1 and 2, details of the refinements in Table 3, and a typical fit is shown in Figure 2.

Results and Discussion

Compression in Silicone Oil. As shown in Figure 3, the unit cell parameter of sil-FAU under pressure in silicone oil shows a quite dramatic and smooth decrease with pressure up to ca. 2.2 GPa. Above this pressure, there is significant peak broadening and this is interpreted as the onset of amorphization. For

(24) Hriljac, J. A.; Eddy, M. M.; Cheetham, A. K.; Donohue, J. A.; Ray, G. J. *J. Solid State Chem.* **1993**, *106*, 66−72.
(25) Attfield, M. P.; Sleight, A. W. *Chem Commun.* **1998**, 601−602.
(26) (a)Villaescusa, L. A.; Lightfoot, P.; Teat, S. J.; Morris, R. E. *J. Am Chem. Soc.* **2001**, *123*, 5453−5459. (b) Lightfoot, P.; Woodcock, M. J.; Villaescusa, L. A.; Wright, P. A. *J. Mater. Chem.* **2001**, *11*, 212−216. (c) Bull, I.; Lightfoot, P.; Villaescusa, L. A.; Bull, L. M.; Gover, R. K. B.; Evans, J. S. O.; Morris, R. E. *J. Am. Chem. Soc.* **2003**, *125*, 4342−4349.
(27) Lemmonier, M.; Fourme, R.; Rosseux, F.; Kahn, R. *Nucl. Instrum. Methods* **1978**, *152*, 173−177.
(28) Smith, G. C. *Synchrotron Rad. News* **1991**, *4*, 24−30.
(29) Hammersley, A. P.; Svensson, S. O.; Hanfland, M.; Fitch, A. N.; Häusermann, D. *High-Pressure Res.* **1996**, *14*, 235−248.
(30) Mao, H. K.; Xu, J.; Bell, P. M. *J. Geophys. Res.* **1986**, *91*, 4673−4676.
(31) Rietveld, H. M. *J. Appl. Crystollogr.* **1966**, *2*, 65−71.
(32) Young, R. A. *The Rietveld Method*; International Union of Crystallography, Oxford University Press: New York, 1995.
(33) Larson, A. C.; Vondreele, R. B. *GSAS.; General Structure Analysis System.* Report LAUR 86-745, Los Alomos National Lab, New Mexico, 1986.

Table 1. Unit Cell Parameters (Å) and Volumes (Å^3) for sil-FAU as a Function of Pressure[a]

sample	*P* (GPa)	a_0	*V*	V/V_0
sil-FAU in methanol:	0.0001	24.268(2)	14279(3)	1.0000
ethanol:water	0.5	24.228(1)	14222(2)	0.9960
ID09	1.0	24.197(1)	14167(2)	0.9922
	1.6	24.182(1)	14141(4)	0.9903
	2.1	24.176(1)	14129(2)	0.9895
	2.7	24.154(1)	14092(2)	0.9869
	3.2	24.132(1)	14053(2)	0.9842
	4.0	24.101(1)	13999(2)	0.9804
	4.8	24.030(1)	13875(2)	0.9717
	5.7	23.941(1)	13721(2)	0.9609
	7.0	23.828(1)	13528(2)	0.9474
	7.9	23.764(20)	13421(3)	0.9399
sil-FAU in methanol:	0.0001	24.242(4)	14246(7)	1.0000
ethanol:water	0.3	24.232(7)	14229(12)	0.9988
X7A	1.1	24.192(4)	14159(7)	0.9938
	2.0	24.128(5)	14046(8)	0.9860
	3.3	24.082(8)	13966(13)	0.9803
	5.2	24.009(11)	13840(19)	0.9714
	6.9	23.848(20)	13549(34)	0.9511
sil-FAU in silicone oil	0.0001	24.242(4)	14246(7)	1.0000
	0.6	24.119(12)	14031(21)	0.9849
X7A	0.9	24.116(6)	14025(10)	0.9845
	1.3	24.032(10)	13879(17)	0.9742
	1.8	23.883(28)	13623(48)	0.9562
	2.4	23.760(11)	13413(18)	0.9415
	0.0001	24.242(4)	14246(7)	1.0000
	0.3	24.189(8)	14153(14)	0.9934
	0.5	24.125(6)	14041(10)	0.9856
	0.9	24.117(14)	14027(20)	0.9846
	1.3	23.996(12)	13817(20)	0.9699

[a] Esd's are in parentheses.

Table 2. Unit Cell Parameters (Å) and Volumes (Å^3) for Na−X as a Function of Pressure[a]

sample	*P* (GPa)	a_0	*V*	V/V_0
Na−X in methanol:	0.0001	24.944(2)	15520(4)	1.0000
ethanol:water	0.15	24.963(3)	15556(6)	1.0023
X7A	0.57	24.895(3)	15429(6)	0.9941
	1.09	24.841(4)	15329(7)	0.9877
	1.77	24.771(4)	15200(7)	0.9794
	2.67	24.693(7)	15056(13)	0.9701
	3.39	24.660(4)	14996(7)	0.9662
	4.21	24.607(4)	14900(7)	0.9600
	5.01	24.535(5)	14769(5)	0.9516
Na−X in silicone oil	0.0001	24.944(2)	15520(4)	1.0000
	0.38	24.856(6)	15356(11)	0.9894
X7A	1.03	24.696(8)	15062(15)	0.9705
	1.58	24.613(5)	14910(9)	0.9607
	1.99	24.522(10)	14746(18)	0.9501
	2.94	24.425(16)	14571(29)	0.9388
	3.92	24.399(48)	14525(86)	0.9359
	5.12	24.316(45)	14377(80)	0.9264

[a] Esd's are in parentheses.

example, the full-width at half-maximum of the (111) peak increases from 0.15° at 2.1 GPa to 0.27° at 2.7 GPa (see the Supporting Information for more details). A similar amorphization pressure has been noted in the absence of a pressure-transmitting fluid.[14] Bulk moduli (Table 4) were calculated from the data using the Murnaghan equation of state with a pressure derivative, K', equal to 4.[34] The derived bulk modulus of 38(2) GPa is typical for zeolite systems, with a reported range of ca. 20−60 GPa. The bulk modulus is virtually identical to that of α-quartz.[35] Although at first this may seem surprising given sil-FAU has less than half the density, this confirms previous work showing that there is no relationship between microporosity, as represented by framework density, and volume compressibility.[36]

Calculated Compressibility. The pure silica framework of sil-FAU and lack of charge-balancing cations or zeolitic water makes it ideal for computational studies. Therefore, simulations were used to investigate the compressibility of sil-FAU in comparison to quartz. Simple energy minimizations over a series of pressures were carried out for pure-silica structures of faujasite and α-quartz. An empirical interatomic potential for tetrahedral SiO_2 structures was used, this was developed by Sanders and Catlow.[37] This potential has been used extensively to study various zeolites, yielding accurate calculated structures and heats of formation.[38] As data for quartz were used to develop this potential, it should be well-suited for the faujasite structure where the average Si−O−Si angle is very similar.[39] The GULP software suite[40] was utilized to perform the constant pressure minimizations in increments of 1 GPa between 0 and 20 GPa, all calculations correspond to a temperature of 0 K.

The behavior of quartz under pressure has been extensively studied.[41,42] Very accurate compressibility data, intended to enable the utilization of quartz as an internal standard in high-pressure experiments, have been measured by Angel and coworkers,[35] and a recent paper by Kim−Zajonz contains a nice summary of the relevant literature.[43] As shown in Figure 3, there is excellent agreement between the observed and predicted data for quartz. There is also reasonable agreement between the observed (silicone oil) and predicted data for sil-FAU, with bulk moduli of 38(2) and 59 GPa, respectively. Although the predicted bulk moduli of sil-FAU is ca. 50% higher than that of quartz, the experimental value is actually essentially identical. This is despite having less than half the density. The comparable compressibility of sil-FAU to quartz does make sense in light of the similar heats of formation observed for quartz and pure silica zeolites.[44]

Compression in Alcohols/Water. When sil-FAU is compressed in a mixture of alcohols/water (16:3:1 methanol:ethanol:water) a much different and peculiar behavior is seen as the solid appears to become *more* compressible with increasing pressure (Figure 4). Upon closer examination, it appears that there are two distinct approximately linear regions with a changeover near 4 GPa. The same affect has been recently reported for scolecite in silicone oil at 6 GPa, this has been attributed to a phase change associated with a reorganization

(34) Angel R. J. *Rev. Minerol. Geochem.* **2001**, *41*, 35−60.
(35) Angel, R. J.; Allan, D. R.; Miletich, R.; Finger, L. W. *J. Appl. Crystallogr.* **1997**, *30*, 461−466.
(36) Gatta, G. D.; Comodi, P.; Zanazzi, P. F. *Micropor. Mesopor. Mater.* **2003**, *61*, 105−115.
(37) Sanders, M. J.; Leslie, M.; Catlow, C. R. A. *J. Chem. Soc., Chem. Commun.* **1984**, 1271−1273.
(38) Henson, N. J.; Cheetham, A. K.; Gale, J. D. *Chem. Mater.* **1994**, *6*, 1647−1650.
(39) Cheetham, A. K.; Bull, L. M.; Henson, N. J. *Surf. Sci. Catal.* **1997**, *105*, 2267−2264.
(40) GULP v 1.1.1 − a computer program for the symmetry adapted simulation of solids, Gale, J. D. *J. Chem. Soc., Faraday Trans.* **1997**, *93*, 629−637.
(41) Mcskimin, H. J.; Andreatch, P., Thurston, R. N. *J. Appl. Phys.* **1965**, *36*, 1624−1701.
(42) Chelikowsky, J. R.; Troullier, N.; Maritins, J. L.; King, H. E., Jr. *Phys. Rev. B* **1991**, *44*, 489−497.
(43) Kim-Zajonz, J.; Werner, S.; Schutz, H. *Z. Kristallogr.* **1999**, *214*, 324−330.
(44) Petrovic, I.; Navrotsky, A.; Davis, M. E.; Zones, S. I. *Chem. Mater.* **1993**, *5*, 1805−1813.

Table 3. Final Refined Atomic Coordinates as a Function of Pressure[a]

P (GPa)	χ^2	atom	*x*	*y*	*z*	fractional occupancy	site symmetry	U_{iso}*100
0.0001	4.508	Si	−0.0527(3)	0.1238(4)	0.0364(3)	1	192 i	0.6(1)
		O(1)	0.0000	−0.1055(6)	0.1055(6)	1	96 h	0.7(3)
		O(2)	−0.0022(6)	−0.0022(6)	0.1392(8)	1	96 g	0.7(3)
		O(3)	0.0765(6)	0.0765(6)	−0.0215(8)	1	96 g	0.7(3)
		O(4)	0.0718(7)	0.0718(7)	0.3152(7)	1	96 g	0.7(3)
0.5	4.483	Si	−0.0517(3)	0.1256(3)	0.0344(3)	1	192 i	0.7(1)
		O(1)	0.0000	−0.1026(5)	0.1026(5)	1	96 h	0.9(2)
		O(2)	−0.0026(6)	−0.0026(6)	0.1409(8)	1	96 g	0.9(2)
		O(3)	0.0755(5)	0.0755(5)	−0.0333(8)	1	96 g	0.9(2)
		O(4)	0.0684(6)	0.0684(6)	0.3175(8)	1	96 g	0.9(2)
		Ow(1)	−0.1250	−0.1250	−0.1250	1	8 a	2.5
		Ow(2)	0.2820(13)	−0.1250	−0.1250	0.739(32)	48 f	2.5
1.0	6.085	Si	−0.0510(3)	0.1259(4)	0.0347(3)	1	192 i	1.0(1)
		O(1)	0.0000	−0.1033(5)	0.1033(5)	1	96 h	1.3(2)
		O(2)	−0.0030(6)	−0.0030(6)	0.1401(8)	1	96 g	1.3(2)
		O(3)	0.0741(7)	0.0741(7)	−0.0312 (9)	1	96 g	1.3(2)
		O(4)	0.0689(7)	0.0689(7)	0.3175 (8)	1	96 g	1.3(2)
		Ow(1)	−0.1250	−0.1250	−0.1250	1	8 a	2.5
		Ow(2)	0.1988	−0.1250	−0.1250	0.748(32)	48 f	2.5
1.6	5.473	Si	−0.0506(3)	0.1255(4)	0.03488(3)	1	192 f	0.9(1)
		O(1)	0.0000	−0.1042(6)	0.1042(6)	1	96 h	1.2(3)
		O(2)	−0.0036(7)	−0.0036(7)	0.1401(8)	1	96 g	1.2(3)
		O(3)	0.0732(6)	0.0732(6)	−0.0294(9)	1	96 g	1.2(3)
		O(4)	0.0698(7)	0.0698(7)	0.3156(9)	1	96 g	1.2(3)
		Ow(1)	−0.1250	−0.1250	−0.1250	1	8 a	2.5
		Ow(2)	0.1857(13)	−0.1250	−0.1250	0.827(33)	48 f	2.5
2.1	4.597	Si	−0.0516(3)	0.1241(3)	0.0358(3)	1	192 i	0.7(2)
		O(1)	0.0000	−0.1046(5)	0.1046(5)	1	96 h	1.4(3)
		O(2)	−0.0027(6)	−0.0027(6)	0.1372(8)	1	96 g	1.4(3)
		O(3)	0.07207(5)	0.07207(5)	−0.0296(8)	1	96 g	1.4(3)
		O(4)	0.06755(6)	0.06755(6)	0.3150(8)	1	96 g	1.4(3)
		Ow(1)	−0.1250	- 0.1250	−0.1250	1	8 a	2.5
		Ow(2)	0.1853(10)	−0.1250	−0.1250	1	48 f	2.5
		Ow(3)	0.2500	0.0000	−0.2500	0.92(4)	32 m	2.5
2.7	4.386	Si	−0.0517(3)	0.1251(4)	0.0359(3)	1	192 i	1.1(2)
		O(1)	0.0000	−0.1030(5)	0.1030(5)	1	96 h	2.0(3)
		O(2)	−0.0029(6)	−0.0029(6)	0.1363(8)	1	96 g	2.0(3)
		O(3)	0.0720(5)	0.0720(5)	−0.0307(8)	1	96 g	2.0(3)
		O(4)	0.0650(6)	0.0650(6)	0.3164(8)	1	96 g	2.0(3)
		Ow(2)	0.1850(10)	−0.1250	−0.1250	1	48 f	2.5
		Ow(3)	0.2500	0.0000	−0.2500	0.66(5)	32 m	2.5
		Ow(4)	−0.1031(11)	−0.1031(11)	−0.1031(11)	0.50	32 m	2.5
3.2	3.583	Si	−0.0524(2)	0.1240(3)	0.0353(3)	1	192 i	1.5(2)
		O(1)	0.0000	−0.1035(5)	0.1035(5)	1	96 h	2.0(3)
		O(2)	−0.0025(5)	−0.0025(5)	0.1320(7)	1	96 g	2.0(3)
		O(3)	0.0730(6)	0.0730(6)	−0.0314(7)	1	96 g	2.0(3)
		O(4)	0.0636(5)	0.0636(5)	0.3189(8)	1	96 g	2.0(3)
		Ow(2)	0.1843(9)	−0.1250	−0.1250	1	48 f	2.5
		Ow(3)	0.2500(2)	0.0000(3)	−0.2500(6)	0.56(4)	32 m	2.5
		Ow(4)	−0.1067(10)	−0.1067(10)	−0.1067(10)	0.5	32 m	2.5
		Ow(5)	−0.0369(11)	−0.0369(11)	−0.2131(11)	0.61(4)	32 m	2.5
4.0	3.309	Si	−0.0529(2)	0.1241(3)	0.0352(3)	1	192 i	1.6(2)
		O(1)	0.0000	−0.1044(5)	0.1044(5)	1	96 h	2.2(3)
		O(2)	−0.0025(5)	−0.0025(5)	0.1313(9)	1	96 g	2.2(3)
		O(3)	0.0731(6)	0.0731(6)	−0.0331(7)	1	96 g	2.2(3)
		O(4)	0.0626(5)	0.0626(5)	0.3180(7)	1	96 g	2.2(3)
		Ow(2)	0.1859(9)	−0.1250	−0.1250	1	48 f	2.5
		Ow(3)	0.2500	0.0000	−0.2500	0.47(4)	32 m	2.5
		Ow(4)	−0.1067(10)	−0.1067(10)	−0.1067(10)	0.5	32 m	2.5
		Ow(5)	−0.0374(11)	−0.0374(11)	−0.2126(11)	0.64(4)	32 m	2.5
4.8	2.756	Si	−0.0523(3)	0.1236(3)	0.0352(3)	1	192 i	2.7(2)
		O(1)	0.0000	−0.1054(5)	0.1054(5)	1	96 h	3.1(3)
		O(2)	−0.0022(5)	−0.0022(5)	0.0343(8)	1	96 g	3.1(3)
		O(3)	0.0727(5)	0.0727(5)	−0.0343(8)	1	96 g	3.1(3)
		O(4)	0.0615(6)	0.0615(6)	0.3169(7)	1	96 g	3.1(3)
		Ow(2)	0.1833(9)	−0.1250	−0.1250	1	48 f	2.5
		Ow(3)	0.2500	0.0000	−0.2500	0.37(4)	32 m	2.5
		Ow(4)	−0.0996(8)	−0.0996(8)	−0.0996(8)	0.69(2)	32 m	2.5
		Ow(5)	−0.0398(11)	−0.0398(11)	−0.2102(11)	0.58(4)	32 m	2.5
		Ow(6)	0.267(4)	−0.0171(34)	−0.0171(34)	0.18(3)	32 m	2.5
5.7	2.745	Si	−0.0525(3)	0.1232(3)	0.03515(3)	1	192 i	3.1(2)
		O(1)	0.0000	−0.1068(5)	0.1068(5)	1	96 h	4.5(3)
		O(2)	−0.0034(6)	−0.0034(6)	0.1352(9)	1	96 g	4.5(3)

Table 3 (Continued)

P (GPa)	χ^2	atom	*x*	*y*	*z*	fractional occupancy	site symmetry	U_{iso}*100
		O(3)	0.0727(6)	0.0727(6)	−0.0328(8)	1	96 g	4.5(3)
		O(4)	0.0625(6)	0.0625(6)	0.3155(8)	1	96 g	4.5(3)
		Ow(2)	0.1818(9)	−0.1250	−0.1250	1	48 f	2.5
		Ow(3)	0.2500	0.0000	−0.2500	0.42(4)	32 m	2.5
		Ow(4)	−0.1008(9)	−0.1008(9)	−0.1008(9)	0.61(2)	32 m	2.5
		Ow(5)	−0.0501(12)	−0.0501(12)	−0.1999(12)	0.58(4)	32 m	2.5
		Ow(6)	0.2607(26)	−0.0107(26)	−0.0107(26)	0.26(4)	32 m	2.5
7.0	2.699	Si	−0.0520(3)	0.1231(4)	0.0343(4)	1	192 i	4.3(2)
		O(1)	0.0000	−0.1095(6)	0.1095(6)	1	96 h	5.2(4)
		O(2)	−0.0075(6)	−0.0075(6)	0.1363(8)	1	96 g	5.2(4)
		O(3)	0.0715(6)	0.0715(6)	−0.0312(8)	1	96 g	5.2(4)
		O(4)	0.0684(7)	0.0684(7)	0.3115(8)	1	96 g	5.2(4)
		Ow(2)	0.1844(9)	−0.1250	−0.1250	1	48 f	2.5
		Ow(3)	0.2500	0.0000	−0.2500	0.40(4)	32 m	2.5
		Ow(4)	−0.1070(17)	−0.1070(17)	−0.1070(17)	0.38(3)	32 m	2.5
		Ow(5)	−0.0696(11)	−0.0696(11)	−0.1804(11)	0.79(3)	32 m	2.5
		Ow(6)	0.2362(19)	0.0138(19)	0.0138(19)	0.37(4)	32 m	2.5
7.9	2.427	Si	−0.0512(3)	0.1220(4)	0.0344(4)	1	192 i	5.3(3)
		O(1)	0.0000	−0.1124(6)	0.1124(6)	1	96 h	6.5(4)
		O(2)	−0.0083(6)	−0.0083(6)	0.1351(9)	1	96 g	6.5(4)
		O(3)	0.0707(6)	0.0707(6)	−0.0276(8)	1	96 g	6.5(4)
		O(4)	0.0701(7)	0.0701(7)	0.3102(8)	1	96 g	6.5(4)
		Ow(2)	0.1822(9)	−0.1250	−0.1250	1	48 f	2.5
		Ow(3)	0.2500	0.0000	−0.2500	0.53(6)	32 m	2.5
		Ow(4)	−0.1133(28)	−0.1133(28)	−0.1133(28)	0.26(3)	32 m	2.5
		Ow(5)	−0.0751(12)	−0.0751(12)	−0.1749(12)	0.85(3)	32 m	2.5
		Ow(6)	0.2403(16)	0.0097(16)	0.0097(16)	0.45(4)	32 m	2.5

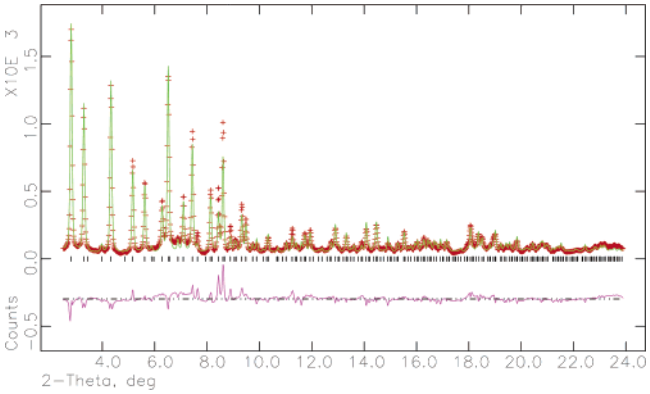

Figure 2. Observed (red), calculated (green), and difference (purple) patterns from the Rietveld refinement using data from sil-FAU at 4.0 GPa with a methanol:ethanol:water pressure-transmitting medium.

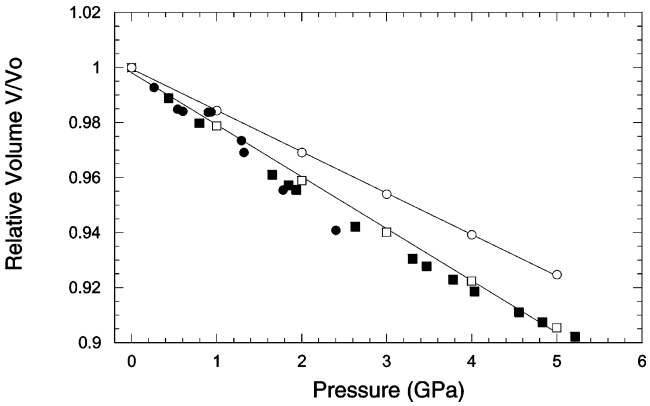

Figure 3. Experimental (closed symbols) and computational (open symbols) normalized volumes of sil-FAU in silicone oil (circles) and quartz[35] (squares) as a function of pressure. The lines are fits to the computational data.

of the hydrogen-bonded network of water within the pores.[9] A similar, but more dramatic, affect was reported for Na−A in water with three volume discontinuities up to 3 GPa. Although attributed to phase transitions, exact details were not reported.[13]

Bulk moduli were independently calculated for the two regions (Table 4). The value for the low pressure region is five times greater than that observed with silicone oil, and nearly three times greater than that of the high-pressure region. Such a dramatic difference in bulk moduli as a function of the pressure-transmitting fluid has been seen before for Na−A and attributed to whether the molecules are small enough to enter the pores during the experiment.[13,14] Interestingly for natrolite, the one case of an aluminosilicate zeolite where high-pressure hydration has been proven, there is no apparent difference in the bulk moduli of the low- and high-pressure phases.[6]

High-Pressure Crystal Chemistry. The data in alcohols/water was of sufficient quality to allow a crystallographic analysis using the Rietveld method. The starting model was known at ambient conditions, i.e., the completely empty framework. The absence of water was confirmed by a TGA analysis, which showed no weight loss up to 600 °C. At the first pressure, it was obvious that additional scattering density needed to be included in the model. Difference Fourier maps were generated, and chemically reasonable sites were included in the models as oxygen atoms whose positions and occupancies were then refined. As it was not possible to refine the temperature factors for these sites, the true errors in the fractional occupancies will be higher than those obtained from the least-squares analysis and should be treated with caution. A total of 6 sites were included, three (Ow(1), Ow(4), and Ow(5) are in the β-cages and three (Ow(2), Ow(3), and Ow(6)) in the supercages. For pressures from 0.5 to 1.6 GPa, site Ow(1) is completely occupied and site Ow(2) progressively fills. At 2.1 GPa, a second site in the supercages, Ow(3), becomes nearly filled. From 2.7 GPa onward, the primary site in the β-cage moves off a special position (Ow(1)) and becomes a partially

Table 4. Bulk Moduli and Volume Compressibilities of Selected Zeolite Frameworks

sample	V_0 (Å^3)	K_0 (GPa)	reference
sil-FAU in alcohols/water, $P \leq 4$ GPa	14251(13)	208(19)	this work[a]
sil-FAU in alcohols/water, $P \geq 4$ GPa	14806(51)	64(3)	this work[a]
sil-FAU in silicone oil, $P \leq 2.4$ GPa	14252(11)	38(2)	this work[a]
Na−X in alcohols/water, $P \leq 5.0$ GPa	15530(17)	89(4)	this work[a]
Na−X in silicone oil, $P \leq 2.0$ GPa	15515(34)	35(2)	this work[a]
Na−A in water		140	14
Na−A in alcohols, $P < 1$ GPa		70	13
Na−A in glycerol		22	14
natrolite in alcohols/water, $P < 1$ GPa		53(1)	6
heulandite in glycerol		27.5(2)	8
scolecite in silicone oil, $P < 5$ GPa		54.6(7)	10
bikitaite in silicone oil		45(1)	11
yugawaralite in silicone oil		34(1)	12

[a] Determined using EOSFIT[31] with all data weighted by their relative uncertainties, esd's are in parentheses.

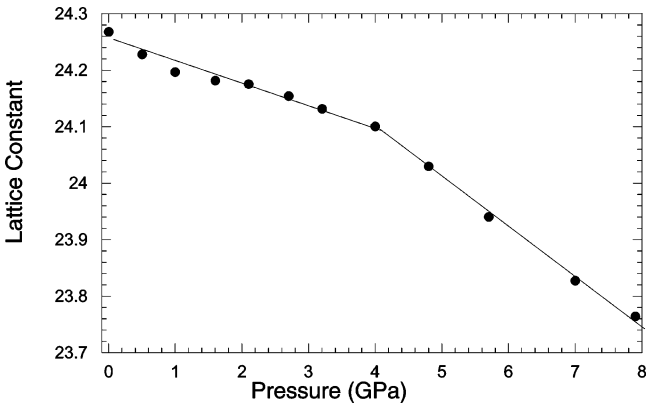

Figure 4. Unit cell constant of sil-FAU in methanol:ethanol:water as determined from the Rietveld analysis. The linear fits to the two regions of compressibility serve as guides to the eye, error bars are smaller than the plotted points.

occupied site nearby, Ow(4). From 3.2 GPa onward, site Ow-(5) in the β-cage becomes occupied and from 4.8 GPa onward, site Ow(6) in the supercages also becomes occupied. There are no distances between sites in the supercages that are less than ca. 4 Å at any pressure. There are distances shorter than the van der Waals contacts between Ow(4) and Ow(5) sites in the β-cages, especially above 7 GPa, but given the partial occupancies these will not be simultaneously occupied. The sum of the site occupancies increases with pressure (Figure 5) and the pore filling of the zeolite reaches saturation near 4.0 GPa. Selected plots of the filling pattern are shown in Figure 6. Given the uncertainty in the nature of the molecules in the pores and large errors associated with the occupancies, it is not possible to state whether the filling is staged, as Figure 5 might imply, or continuous. We note, however, that the curve does resemble a typical adsorption isotherm.

The Si−O bond length data (Table 5) shows the bond distances within the framework vary little with pressure. Similarly, the mean O−Si−O bond angle (Table 6 and Figure 7) remains nearly constant with pressure. However, significant changes do occur in individual Si−O−Si angles above ~4.0 GPa. The angles about O(2) and O(3) remain approximately constant while the Si−O(1)−Si bond angle decreases to the same extent as the Si−O(4)−Si angle increases. This distorts both the sodalite units and the connecting double 6 rings (D6R) (Figure 1). The O(1) atoms bridge the two halves of the D6R, therefore it contracts, and the O(4) atoms bridge three of the

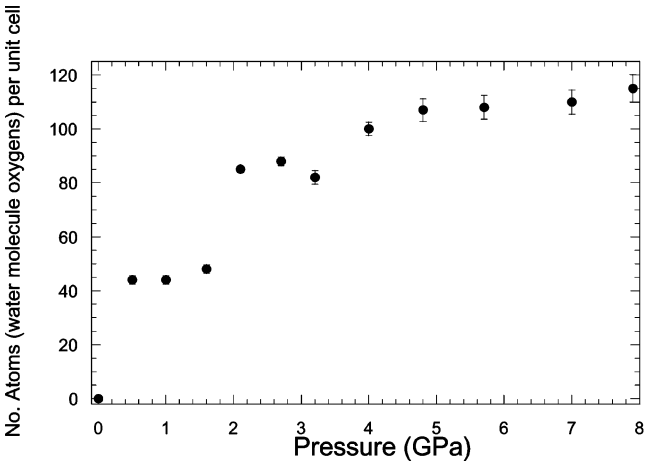

Figure 5. Trend in pore filling with pressure for sil-FAU using methanol:ethanol:water as a pressure-transmitting medium.

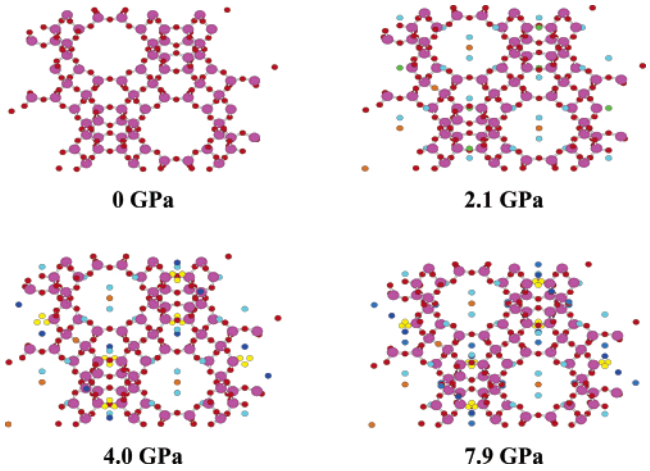

Figure 6. Pore filling of sil-FAU with pressure.

Table 5. Silicon−Oxygen Bond Lengths (Å) for sil-FAU as a Function of Pressure[a]

P (GPa)	Si–O(1)	Si–O(2)	Si–O(3)	Si–O(4)	mean
0.0001	1.6184(3)	1.5880(3)	1.6849(3)	1.6029(3)	1.614
0.5	1.590(9)	1.535(9)	1.631(9)	1.633(11)	1.597
1.0	1.614(9)	1.516(9)	1.646(10)	1.621(12)	1.599
1.6	1.631(10)	1.510(9)	1.650(11)	1.610(12)	1.600
2.1	1.617(9)	1.537(8)	1.623(10)	1.639(11)	1.604
2.7	1.604(8)	1.530(8)	1.630(10)	1.649(12)	1.603
3.2	1.580(7)	1.524(7)	1.611(9)	1.700(11)	1.604
4.0	1.576(8)	1.526(8)	1.604(9)	1.703(11)	1.602
4.8	1.591(8)	1.524(8)	1.581(9)	1.718(11)	1.604
5.7	1.598(9)	1.521(8)	1.579(10)	1.702(12)	1.600
7.0	1.627(11)	1.489(9)	1.595(11)	1.628(11)	1.585
7.9	1.684(11)	1.471(9)	1.595(11)	1.631(10)	1.595

[a] Esd's are in parentheses.

six edges of the hexagonal faces of the sodalite units and therefore these edges expand. The affect of pressure on the D6R unit has been noted before as the main distortion observed by IR spectroscopy under pressure in the absence of a pressure-transmitting medium, prior to amorphization.[21] This is fully consistent with our results as at pressures above 4 GPa pore filling is completed, and the interior of the zeolite is no longer accessible for small molecules.

The results of the Rietveld refinements allow us to explain the unusual compressibility behavior of sil-FAU. This material has a neutral framework and should be hydrophobic, as

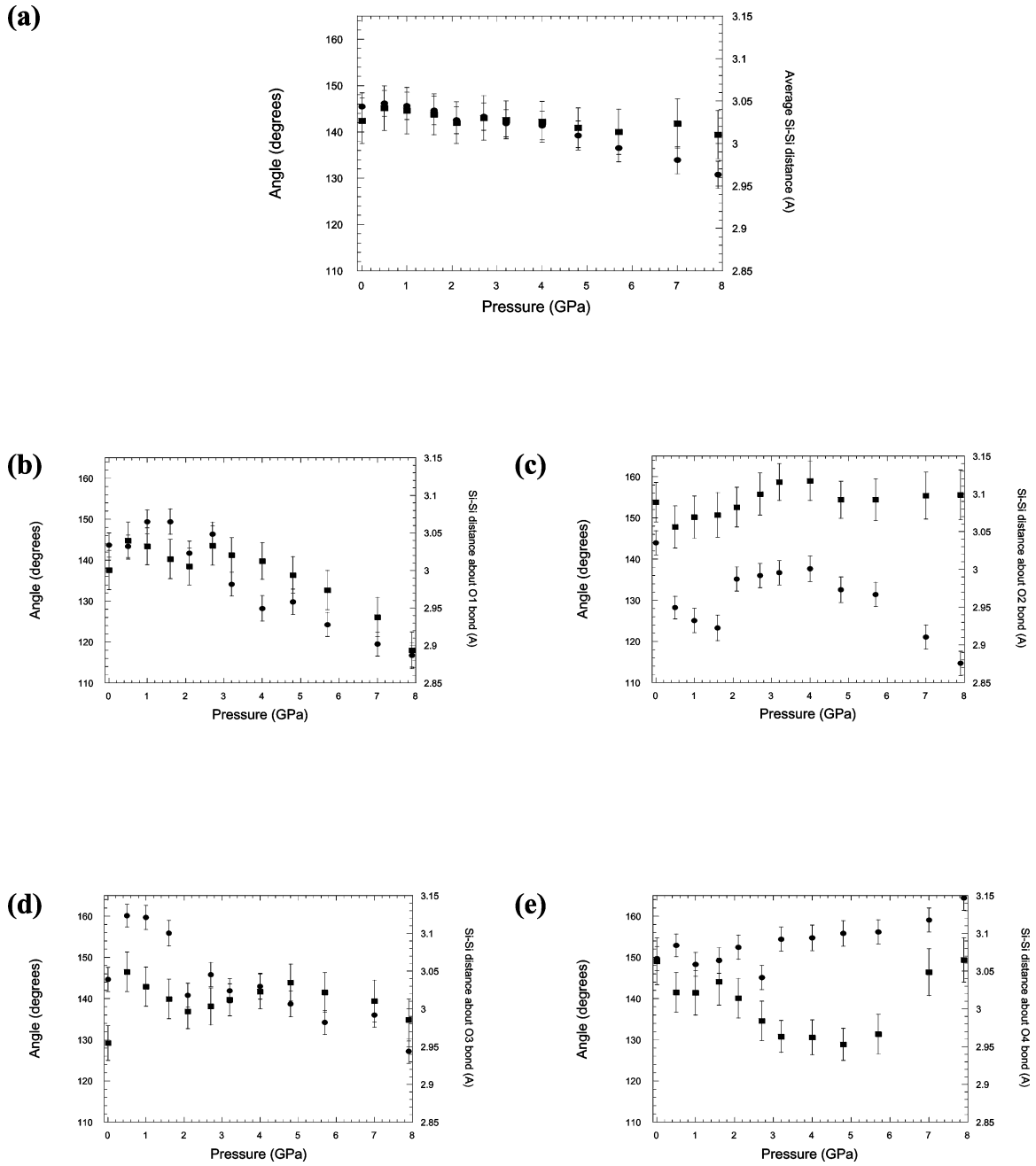

Figure 7. Silicon−oxygen−silicon bond angles (squares) and silicon−silicon distances (circles) as a function of pressure: (a) mean values; (b) Si−O(1)−Si; (c) Si−O(2)−Si; (d) Si−O(3)−Si; and (e) Si−O(4)−Si.

confirmed by the absence of any water in its pores at ambient conditions by TGA. However, pressure is able to drive molecules into the pores. Up to 4 GPa, pressure-induced pore filling is the principal process that occurs. The zeolite has a low apparent compressibility (high bulk modulus), which is based solely on the unit cell size which is dictated by the framework as the force of the applied pressure is pushing molecules into the solid and reducing the volume of the fluid. After the filling of the pores, a larger compressibility is seen as the pressure is now predominantly affecting and distorting the silicate framework. The difference between the compression behavior in silicone oil and alcohol/water is due to the ability of the pressure medium to penetrate the pores and channels of the faujasite framework. Silicone oil cannot penetrate into the zeolite, therefore all pressure exerted on the zeolite goes directly

Table 6. Silicon−Oxygen−Silicon Bond Angles (deg) for sil-FAU as a Function of Pressure[a]

P (GPa)	Si–O(1)–Si	Si–O(2)–Si	Si–O(3)–Si	Si–O(4)–Si	mean
0.0001	137(2)	154(2)	129(1)	149(2)	142
0.5	145(2)	148(2)	147(2)	142(2)	145
1.0	143(2)	150(2)	143(2)	141(2)	142
1.6	140(2)	151(2)	140(2)	144(2)	144
2.1	139(2)	153(2)	137(1)	140(2)	142
2.7	144(2)	156(2)	138(2)	135(2)	143
3.2	141(1)	159(2)	140(1)	131(1)	143
4.0	140(2)	159(2)	142(1)	131(1)	142
4.8	136(2)	154(2)	144(2)	129(1)	141
5.7	133(2)	154(2)	142(2)	131(2)	140
7.0	126(2)	155(2)	139(2)	146(2)	142
7.9	118(2)	156(2)	135(2)	149(2)	139

[a] Esd's are in parentheses.

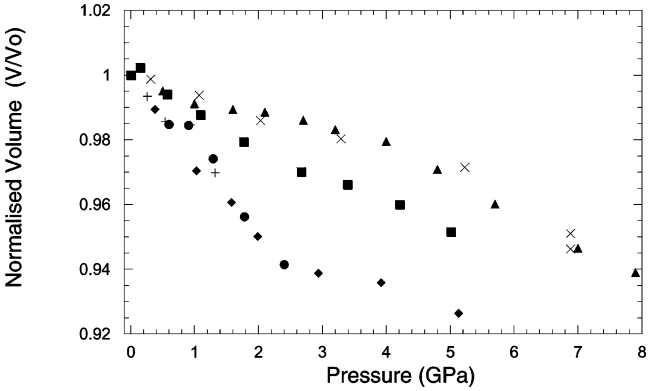

Figure 8. Normalized volume as a function of pressure for FAU zeolites, all data from X7A unless noted. sil-FAU in silicone oil as circles and plusses; Na−X in silicone oil as diamonds; sil-FAU in alcohols/water as triangles (ESRF) and crosses; and Na−X in alcohols/water as squares.

into compression of the framework and leads to a low bulk moduli. The changes in bond angles predicted by the simulations (for the case of empty pores) are very different than that observed experimentally in the case of filled pores. These differences are likely due to distinct compression mechanisms for the empty pores case, despite the fact that higher total compressions are observed.

Zeolite Na−X. Preliminary experiments have also been conducted on a sample of Na−X. The volume changes are similar to those observed for sil-FAU in alcohols/water and identical for silicone oil (Figure 8). The difference between the two systems in alcohols/water can be attributed to the different compositions of the zeolites at ambient conditions: sil-FAU has completely empty pores whereas Na−X contains water and charge-balancing sodium cations. Therefore in zeolite Na−X, more of the initial applied force goes into compressing the framework rather than pushing fluid into the pores, leading to a higher initial compressibility in alcohols/water and a bulk modulus of 91(2) GPa. In silicone oil, a nonpenetrating fluid, the two FAU zeolites show identical compression as the intrapore contents are unaffected by pressure. The intrinsic bulk modulus of the FAU framework is 38(2) GPa, and prior to amorphization it is not affected by the Si/Al ratio of the framework or changes of species in the pores.

Conclusions

Rietveld refinement using synchrotron X-ray powder diffraction data on sil-FAU up to 8 GPa shows pore filling of the 'hydrophobic' faujasite framework as the primary feature in alcohols/water below 4 GPa. Above 4 GPa the primary response of the zeolite is a distortion of the framework involving the sodalite and D6R units. The behavior under pressure is dependent on the pressure-transmitting medium, the filling of the pores does not occur when silicone oil is used. The nature of the molecules entering the zeolite is as yet unknown, and further investigations are required to determine whether water or methanol is "squeezed" into the zeolite. Preliminary experiments for Na−X reveal similar, but less dramatic, behavior in alcohols/water and identical behavior when using silicone oil. The intrinsic bulk modulus of the FAU framework, 38(2) GPa, is that determined using a nonpenetrating pressure medium and is essentially identical to that of α-quartz. Energy minimization calculations predict this value reasonably well, confirming their use for siliceous zeolite frameworks under pressure.

Acknowledgment. This work was supported by the provision of studentship funding by the EPSRC (M.C.) and an LDRD at Brookhaven (Y.L.). We thank Dr Julian Gale for helpful discussions, the ESRF for provision of beamtime, Dr M Hanfland (ESRF) for help with the data collection and reduction, and Dr. J. Hu of the Geographical Lab of the Carnegie Institute for access to the ruby laser system at NSLS beamline X17c. The research was carried out in part at the NSLS at BNL, supported by the U.S. DOE under contract DE-AC02-98CH10886.

Supporting Information Available: Details (volume, Si−O distances, O−Si−O and Si−O−Si angles, fractional atomic coordinates) of the computer simulations and a graph of the observed full width at half-maximum of the (111) peak as a function of pressure. This material is available free of charge via the Internet at http://pubs.acs.org.

JA048685G